Bioorganic & Medicinal Chemistry 17 (2009) 3763–3769

Contents lists available at ScienceDirect

Bioorganic & Medicinal Chemistry

journal homepage: www.elsevier.com/locate/bmc

Anti-inflammatory cembranolides from the soft coral *Lobophytum durum*

Shi-Yie Cheng [a], Zhi-Hong Wen [a], Shang-Kwei Wang [b], Shu-Fen Chiou [a], Chi-Hsin Hsu [a,d], Chang-Feng Dai [c], Chang-Yih Duh [a,d,*]

[a] Department of Marine Biotechnology and Resources, National Sun Yat-sen University, Kaohsiung 804, Taiwan
[b] Department of Microbiology, Kaohsiung Medical University, Kaohsiung 807, Taiwan
[c] Institute of Oceanography, National Taiwan University, Taipei, Taiwan
[d] Center of Asia-Pacific Marine Researches, National Sun Yat-sen University, Kaohsiung, Taiwan

ARTICLE INFO

Article history:
Received 13 March 2009
Revised 23 April 2009
Accepted 24 April 2009
Available online 3 May 2009

Keywords:
Lobophytum durum
Cembranolides
Antibacterial activities
Anti-inflammatory effects
HCMV endonuclease activity

ABSTRACT

Chemical investigation of the soft coral *Lobophytum durum* resulted in the isolation of seven new cembranolides, durumolides F–L (**1**–**7**), as well as one previously characterized cembranolides, sinularolide D (**8**). The molecular structures of these isolated metabolites were determined mainly through NMR techniques and HRESIMS analysis. Moreover, the absolute configurations of **1** and **5** were established by application of modified Mosher's method. The antibacterial activities, anti-inflammatory effects, and anti-HCMV (Human cytomegalovirus) endonuclease activity of metabolites **1**–**8** were also evaluated in vitro. Anti-inflammatory activity of metabolites **1** and **6** (10 μM) significantly reduced the levels of the iNOS protein to 0.8 ± 0.6% and 5.7 ± 2.2%, respectively, and COX-2 protein to 47.8 ± 9.0% and 71.6 ± 5.8%, respectively. Metabolites **1**–**8** (100 μg/disk) exhibited weak antibacterial activity against *Salmonella enteritidis*.

1. Introduction

Soft corals belonging to the genus *Lobophytum* (Alcyoniidae) have been well recognized as a rich source of macrocyclic cembrane-type diterpeniods and their cyclized derivatives.[1–19] Previous bioassay results of some cembranoid analogues have been shown to exhibit diverse biological properties such as cytotoxic,[2–6,19] anti-inflammatory,[18] and antibacterial activities.[18] The chemical investigations for bioactive constituents prompted us to explore the secondary metabolites of the soft coral *Lobophytum durum* (Tixier-Durivault, 1956). We have previously isolated five new cembranolides, named as durumolides A–E, from the acetone-soluble of the organism.[18] Our continuous chemical examination of the secondary of this soft coral led to the isolation of seven new cembranolides, durumolides F–L (**1**–**7**), and sinularolide D (**8**).[20] Herein, we describe the isolation, structural elucidation, anti-inflammatory effects, antibacterial activities, and inhibition assay of HCMV endonuclease activity of these metabolites.

2. Results and discussion

The acetone extract of the soft coral *L. durum* was partitioned between EtOAc and H_2O to afford the EtOAc-soluble portion, which was then subjected to column chromatography on silica gel. The fractions containing cembranolides were selected for further purification by C-18 HPLC to obtain metabolites **1**–**8** (see Section 3).

Durumolide F (**1**) was isolated as a colorless oil. Its HRESIMS (*m*/*z* 415.2097, $[M+Na]^+$) and NMR spectroscopic data (Tables 1 and 2) established the molecular formula $C_{22}H_{32}O_6$, implying seven degrees of unsaturation. The IR spectrum of **1** at 1767 and 1665 cm^{-1} demonstrated absorption bands diagnostic of an α-methylene-γ-lactone functionality. This was further indicated from the ^1H NMR signals at δ_H 6.29 (1H, d, J = 1.3 Hz) and 5.68 (1H, d, J = 1.9 Hz) and ^{13}C NMR signals at δ_C 170.2 (qC, C-16), 139.7 (qC, C-15), 123.2 (CH_2, C-17), 81.8 (CH, C-14), and 42.5 (CH, C-1).[18] A strong IR spectrum absorption at 1735 cm^{-1} indicated the presence of an acetoxy group. A secondary hydroxyl and a tertiary hydroxyl were recognized as being present in **1** from its ^1H NMR signals at δ_H 3.49 (1H, br t, J = 8.3 Hz) and ^{13}C NMR signals at δ_C 70.9 (CH, C-3) and 75.2 (qC, C-4), as well as from a broad IR absorption at 3462 cm^{-1}. The ^{13}C NMR signals at δ_C 124.2 (CH, C-7), 136.7 (qC, C-8), 128.4 (CH, C-11), and 130.3 (qC, C-12) were assigned two trisubstituted double bonds in **1**. The above functionalities account for five of the seven degrees of unsaturation, suggesting a bicyclic structure in **1**. By interpretation of ^1H–^1H COSY correlations, it was possible to establish three partial structures of consecutive proton systems extending from H-3 to H_2-13 through H_2-2, H-1 and H-14, from H_2-5 to H-7, and from H-9 to H-11, as well as long-range COSY correlations between H-1/H_2-17, H_3-19/H-7, and H_3-20/H-11. Moreover, the connectivities of these partial structures were

* Corresponding author. Tel.: +886 7 5252000x5036; fax: +886 7 5255020.
E-mail address: yihduh@mail.nsysu.edu.tw (C.-Y. Duh).

0968-0896/$ - see front matter © 2009 Elsevier Ltd. All rights reserved.
doi:10.1016/j.bmc.2009.04.053

Table 1
^{1}H NMR spectroscopic data of metabolites **1–3**

H#	**1**[a]	**2**[b]	**3**[a]
1	2.97 m	2.63 m	2.75 m
2	a: 1.93 m	a: 2.07 m	1.96 m
	b: 1.64 m	b: 2.00 m	
3	3.49 br t (8.3)[c]	5.22 dd (8.0, 5.5)[c]	5.17 dd (7.4, 5.1)[c]
5	a: 1.86 m	a: 1.76 m	a: 1.83 m
	b: 1.68 m	b: 1.64 m	b: 1.70 m
6	2.20 m	a: 2.25 m	2.20 m
		b: 2.20 m	
7	5.26 br t (6.9)	5.08 br t (6.5)	5.06 br t (6.8)
9	2.18 m	2.20 m	2.20 m
10	a: 2.39 m	a: 2.46 m	a: 2.40 m
	b: 2.17 m	b: 2.25 m	b: 2.25 m
11	5.09 br d (4.9)	5.44 dd (7.5, 3.0)	5.54 br d (6.6)
13	a: 2.57 br d (12.4)	3.96 d (8.5)	5.10 d (8.5)
	b: 2.16 m		
14	4.32 dt (9.9, 2.8)	4.24 dd (8.5, 6.0)	4.33 dd (8.5, 4.8)
17	a: 6.29 d (1.3)	a: 6.29 d (2.5)	a: 6.29 d (1.9)
	b: 5.68 d (1.9)	b: 5.85 d (2.5)	b: 5.78 d (1.3)
18	a: 4.20 d (11.8)	a: 4.14 d (12.0)	a: 4.13 d (11.8)
	b: 4.13 d (11.8)	b: 4.05 d (12.0)	b: 4.05 d (11.8)
19	1.64 s	1.67 s	1.67 s
20	1.76 s	1.74 s	1.74 s
18-OAc	2.11 s	2.12 s	2.12 s
3-OAc		2.06 s	2.07 s
13-OAc			2.08 s

[a] Spectra were measured in $CDCl_3$ (300 MHz).
[b] Spectra were measured in $CDCl_3$ (500 MHz).
[c] *J* values (in Hz) are in parentheses.

Table 2
^{13}C NMR spectroscopic data of metabolites **1–7**

C#	**1**[a]	**2**[b]	**3**[a]	**4**[a]	**5**[a]	**6**[c]	**7**[c]
1	42.5 (CH)[d]	39.3 (CH)[d]	39.9 (CH)[d]	41.9 (CH)[d]	42.3 (CH)[d]	42.6 (CH)[d]	42.3 (CH)[d]
2	36.4 (CH_2)	33.2 (CH_2)	33.6 (CH_2)	31.3 (CH_2)	31.9 (CH_2)	34.9 (CH_2)	34.8 (CH_2)
3	70.9 (CH)	73.3 (CH)	73.3 (CH)	62.2 (CH)	63.4 (CH)	58.5 (CH)	59.1 (CH)
4	75.2 (qC)	75.7 (qC)	75.5 (qC)	60.3 (qC)	60.2 (qC)	63.3 (qC)	65.6 (qC)
5	34.2 (CH_2)	33.4 (CH_2)	33.6(CH_2)	32.3 (CH_2)	38.0 (CH_2)	30.5 (CH_2)	26.0 (CH_2)
6	21.7 (CH_2)	22.7 (CH_2)	22.5 (CH_2)	23.9 (CH_2)	24.4 (CH_2)	21.4 (CH_2)	21.2 (CH_2)
7	124.2 (CH)	122.3 (CH)	122.9 (CH)	128.7 (CH)	124.5 (CH)	127.1 (CH)	126.3 (CH)
8	136.7 (qC)	136.8 (qC)	136.3 (qC)	137.7 (qC)	134.6 (qC)	133.9 (qC)	134.7 (qC)
9	37.6 (CH_2)	37.4 (CH_2)	37.5 (CH_2)	77.4 (CH)	38.7 (CH_2)	37.5 (CH_2)	37.6 (CH_2)
10	24.9 (CH_2)	24.7 (CH_2)	24.8 (CH_2)	33.2 (CH_2)	24.8 (CH_2)	25.9 (CH_2)	25.6 (CH_2)
11	128.4 (CH)	132.1 (CH)	133.7 (CH)	128.1 (CH)	132.4 (CH)	145.4 (CH)	145.5 (CH)
12	130.3 (qC)	131.7 (qC)	129.6 (qC)	130.7 (qC)	131.7 (qC)	135.8 (qC)	136.2 (qC)
13	46.1 (CH_2)	80.4 (CH)	80.1 (CH)	79.9 (CH)	81.3 (CH)	195.3 (qC)	194.8 (qC)
14	81.8 (CH)	84.4 (CH)	82.2 (CH)	79.4 (CH)	82.3 (CH)	77.2 (CH)	76.4 (CH)
15	139.7 (qC)	139.8 (qC)	138.9 (qC)	137.9 (qC)	138.7 (qC)	137.0 (qC)	136.3 (qC)
16	170.2 (qC)	168.6 (qC)	168.5 (qC)	168.8 (qC)	169.1 (qC)	169.8 (qC)	169.1 (qC)
17	123.2 (CH_2)	124.0 (CH_2)	123.8 (CH_2)	124.3 (CH_2)	124.3 (CH_2)	122.9 (CH_2)	123.6 (CH_2)
18	67.7 (CH_2)	66.8 (CH_2)	66.9 (CH_2)	63.6 (CH_2)	16.7 (CH_3)	63.8 (CH_2)	199.3 (CH)
19	17.0 (CH_3)	17.2 (CH_3)	17.1 (CH_3)	11.2 (CH_3)	15.5 (CH_3)	15.7 (CH_3)	15.4 (CH_3)
20	17.5 (CH_3)	12.6 (CH_3)	13.2 (CH_3)	13.3 (CH_3)	12.2 (CH_3)	11.6 (CH_3)	11.7 (CH_3)
18-OAc	20.9 (CH_3)	20.9 (CH_3)	21.0 (CH_3)	20.7 (CH_3)			
	171.7 (qC)	171.2 (qC)	171.2 (qC)	170.7 (qC)			
3-OAc		21.1 (CH_3)	21.0 (CH_3)				
		170.3 (qC)	170.3 (qC)				
13-OAc			20.9 (CH_3)	21.0 (CH_3)			
			169.9 (qC)	169.5 (qC)			

[a] Spectra were measured in $CDCl_3$ (75 MHz).
[b] Spectra were measured in $CDCl_3$ (125 MHz).
[c] Spectra were measured in $CDCl_3$ (100 MHz).
[d] Multiplicities are deduced by HSQC and DEPT experiments.

further established by the HMBC correlations (Fig. 1). The long-range ^{1}H–^{13}C correlations observed from H_2-18 to C-3, C-4, C-5, and the carbonyl carbon of 18-OAc indicated the position of the acetoxy group at C-18. In addition, the above HMBC correlations also led the assignment of the two hydroxyls at C-3 and C-4, respectively. The locations of the two double bonds at C-7/C-8 and C-11/C-12 were clarified by analysis of the HMBC correlations from H_3-19 to C-7, C-8, and C-9 and from H_3-20 to C-11, C-12, and C-13. Thus, the gross structure of durumolide F was unmistakably assigned as **1**, possessing an α-methylene-γ-lactone ring fused to a 14-membered ring at C-1 and C-14.

The determination of the configurations of an α-methylene-γ-lactone ring fused to a 14-membered ring based on the coupling constant between the lactonic methine protons ($^3J_{1,14}$) is dubious.[19] The relative stereochemistry of **1** assigned by NOESY spectrum was compatible with those of **1** offered by computer modeling (Fig. 2), in which the close contacts of atoms calculated in space were consistent with the NOESY correlations. The calculated torsion angles for a *trans*-fused α-methylene-γ-lactone of **1** are identical to those of an analogue, deacetyl-13-hydroxy lobolide,[13] which were determined by an X-ray crystallographic analysis.[18] This suggests that the preferred conformation for a *trans*-fused α-methylene-γ-lactone of **1** is generally in agreement with its crystal structure. Also, it is noted that all the calculated distances between the protons in this computer-generated perspective model that show NOE correlations are less than 3.0 Å. The geometry of the trisubstituted olefins was assigned as *E* based on the γ-effect of the olefinic methyl signals for C-19 and C-20 (less than 20 ppm)[21] and the NOESY correlations between H-7 and H_2-9, H_2-6 and H_3-19, H-11 and H_2-13, and H_2-10 and H_3-20. The NOESY correlations (Fig. 2) between H-1/H-2b (δ_H 1.64), H-1/H-3, H-1/H-11, H-1/H-13b (δ_H 2.16), H-18a (δ_H 4.20)/H-5b (δ_H 1.68), H-3/H-7, H-7/H-6, H-7/H-9, H-11/H-10b (δ_H 2.17), H-3/H-2b, H-14/H-2a (δ_H 1.93), H-14/H_3-20, and H-2b/H-17b (δ_H 5.68) confirmed the geometry of the *trans*-fused lactone ring and indicated that H-1, H-2b, H-3, H-11, and H-13b are located on the same side of the ring system, whereas H-2a, H-13a, H-14, H_2-18, and H_3-20 are oriented toward the opposite side. The absolute stereochemistry of **1** was determined by spectroscopic method for secondary alcohols.[22] Analysis of the $\Delta\delta_{S-R}$ values (Fig. 3) according to the Mosher's model pointed to an *S* configuration for C-3 of **1**, because H-1, H_2-2, and H-14 of (*S*)-MTPA ester **1a** were more shielded by the phenyl ring of MTPA products. From the above observations, **1** was elucidated as (1*R*,3*S*,4*S*,14*S*,7*E*,11*E*)-18-acetoxy-3,4-dihydroxycembra-7,11,15(17)-trien-16,14-olide.

Durumolide G (**2**), appeared as a colorless oil, was isolated as the most polar metabolite. Its HRESIMS (*m/z* 473.2153, $[M+Na]^+$) and NMR spectroscopic data (Tables 1 and 2) established the molecular formula $C_{24}H_{34}O_8$, implying the existence of eight degrees of unsaturation. The NMR spectroscopic data of metabolite **2** were consistent with a cembranolide skeleton having an α-methylene-γ-lactone moiety, corresponding to exomethylene protons at δ_H 6.29 (1H, d, *J* = 2.5 Hz) and 5.85 (1H, d, *J* = 2.5 Hz) that correlated to the methine carbon at δ_C 39.3 (C-1), the quaternary olefinic carbon at δ_C 139.8 (C-15), and the lactone carbonyl signal at δ_C 168.8 (C-16) in the HMBC spectrum. Two trisubstituted double bonds at C-7 and C-8 [δ_H 5.08 (br t, *J* = 6.5 Hz, 1H); δ_C 136.8 (qC) and 122.3 (CH)], and C-11 and C-12 [δ_H 5.44 (dd, *J* = 7.5, 3.0 Hz, 1H); δ_C 131.7 (qC) and 132.1 (CH)] were evidenced by HMBC correlations of H_3-19 to C-7, C-8, and C-9 and of H_3-20 to C-11, C-12, and C-13. In addition to a lactone carbonyl, the ^{13}C NMR data exhibited two carbonyl signals. The carbonyl signal at δ_C 170.3 was attributed to the acetate moiety linked to C-3, as indicated by HMBC correlations of H-3 to the carbonyl carbon of 3-OAc. The other acyl (δ_C 171.2) was assigned to C-18, as indicated by the HMBC correlations of two isolated oxymethylene protons (δ_H 4.14 and 4.05) to the carbonyl carbon of 18-OAc. Furthermore, the HMBC spectrum was used to locate two hydroxyl substitutions at C-4 and C-13. The stereochemistry of **2** assigned by NOESY spectrum was compatible with that of **1** offered by computer-generated perspective model using MM2 force field calculations, in which the close contacts of atoms calculated space were consistent with NOESY correlations. The NOESY spectrum and the conformer generated by Chem3D Pro 9.0 indicated that **2** possessed the same configuration as **1** at the C-1, C-3, C-4, and C-14 stereocenters. From the NOESY spectrum

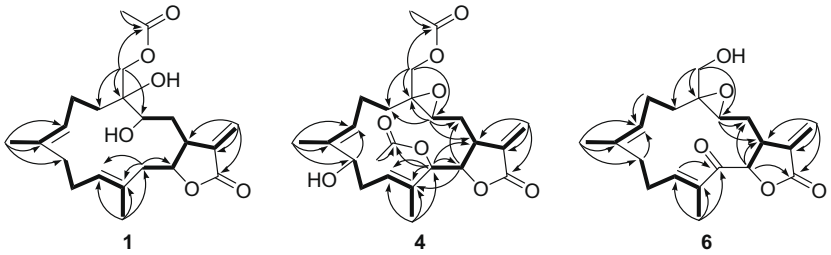

Figure 1. ^{1}H–^{1}H COSY (—) and key HMBC (→) correlations of **1**, **4**, and **6**.

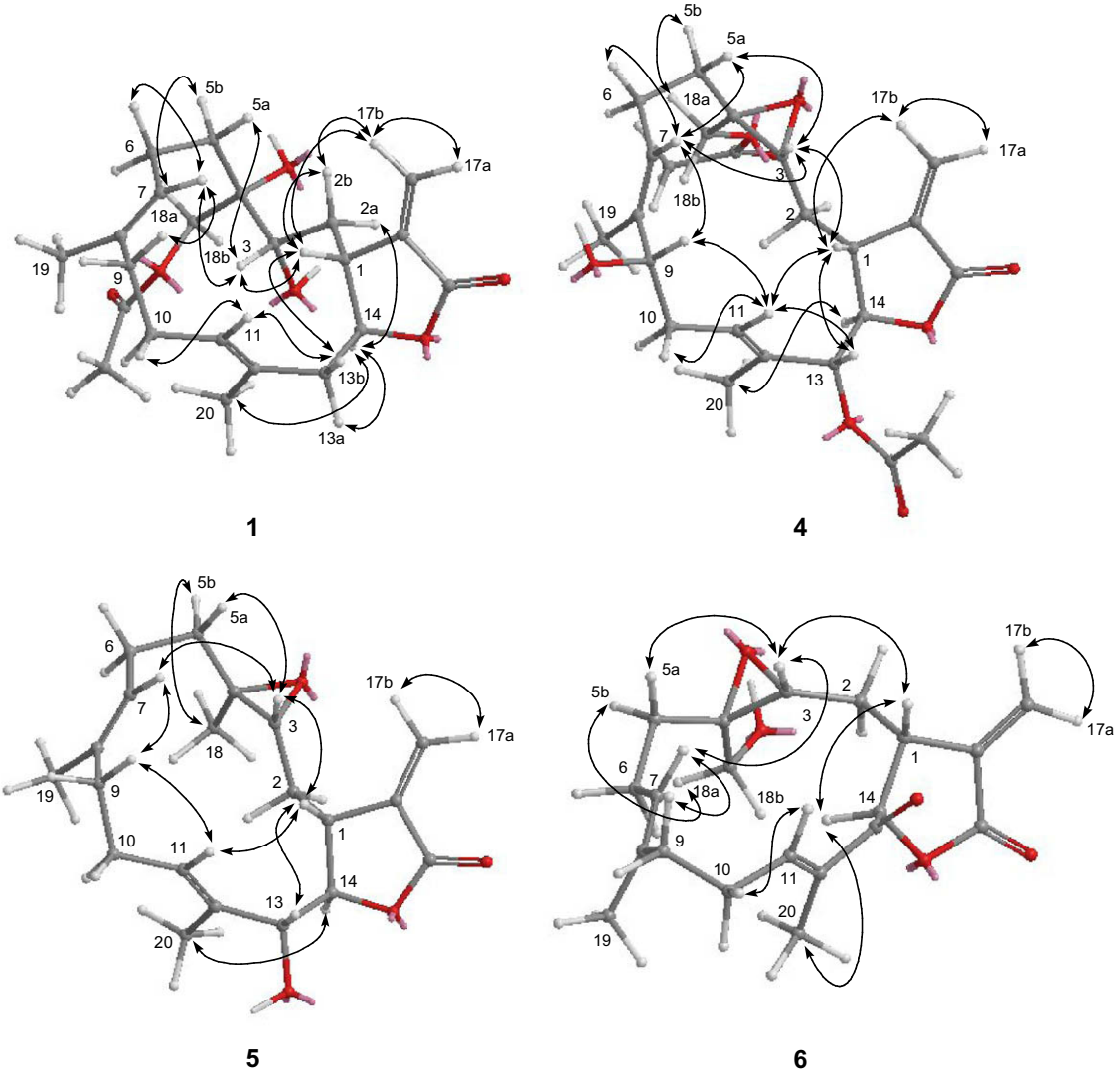

Figure 2. Key NOE correlations and computer-generated perspective model using MM2 force field calculations for **1** and **4**–**6**.

of **2**, H-13 was found to show the NOE correlations with both H-1 and H-11, indicating the R^{*}-configuration of the secondary hydroxyl attached at C-13. The NOE correlations between H_2-18/H_2-2, H_3-19/H_2-6, H_3-20/H_2-10, H-3/H_2-5, H_2-9/H-7, and H-11/H-13, respectively, reflected the *E* geometry of the two trisubstituted double bonds in the molecule. According to the aforementioned observations and other detailed NOESY correlations, the structure of metabolite **2** was unambiguously determined as (1R^{*},3S^{*},4S^{*},13R^{*},14S^{*},7*E*,11*E*)-3,18-diacetoxy-4,13-dihydroxycembra-7,11,15(17)-trien-16,14-olide.

Durumolide H (**3**) was obtained as a colorless oil, which analyzed for the molecular formula $C_{26}H_{36}O_9$ by HRESIMS coupled with the DEPT and ^{13}C NMR spectroscopic data (Table 2). Analysis of the COSY and HMBC correlations were diagnostic in determining that the gross framework of durumolide H, containing a 14-membered ring fused to an α-methylene-γ-lactone ring, was assigned as **3**. The structure of **3** was identical to that of **2** with the exception that the hydroxy group attached to C-13 was replaced by an acetoxy group. This was confirmed through HMBC correlations from H-13 to C-1, C-14, C-20, and the carbonyl carbon of 13-OAc. Metabo-

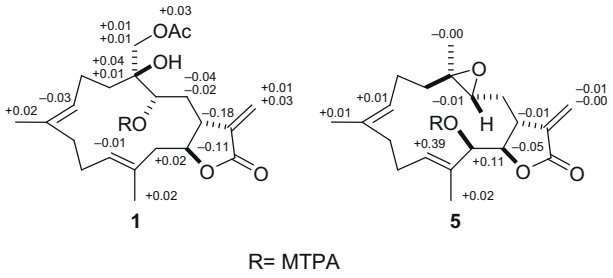

Figure 3. Selected ^{1}H NMR $\Delta\delta_{S-R}$ values in ppm for the *S*- and *R*-MTPA esters of **1** and **5** in $CDCl_3$.

lite **3** is simply an acetylation product of **2**. All the NMR spectroscopic data of **3**, assigned by COSY, HMBC, and NOESY correlations, were satisfactorily consistent with the structure shown as (1*R**,3*S**,4*S**,13*R**,14*S**,7*E*,11*E*)-3,13,18-triacetoxy-4-hydroxycembra-7,11,15(17)-trien-16,14-olide.

The positive HRESIMS of **4** exhibited a pseudo molecular ion peak at *m*/*z* 471.1993 $[M+Na]^+$, corresponding to the molecular formula $C_{24}H_{32}O_8$ and nine degrees of unsaturation. Both the ^{1}H and ^{13}C NMR spectroscopic data (Tables 2 and 3) demonstrated the presences of an α-methylene-γ-lactone ring, two acetate units, an epoxide, and two trisubstituted double bonds, which accounted for eight degrees of nine unsaturations and were suggestive of a tricyclic cembranolide bearing an α-methylene-γ-lactone moiety and an epoxide ring. The lactone carbonyl signal at δ_C 168.8 (C-16) was assigned to an α-methylene-γ-lactone ring together with the oxymethine at δ_C 79.4 (C-14) and the methine carbon at δ_C 41.9 (C-1). The NMR signals at δ_H 6.33 and 6.03 as well as at δ_C 124.3 were ascribed to an exocyclic methylene group and correlated to C-1, C-15, and C-16, thereby proving the presence of a 14,16-lactone ring (Fig. 1). Two acetates resonated at δ_H 2.15 and 2.12 (each 3H, s) and δ_C 170.7 (C), 169.5 (C), 20.7 (CH_3), and 21.0 (CH_3). Meanwhile, the oxymethine observed at δ_H 5.28 (H-13), and the oxymethylene at δ_H 4.41 (H-18a) and 3.85 (H-18b) exhibited HMBC correlations to two acetoxy carbonyls, proving acetyloxy substitution at these positions, and was confirmed by the COSY correlations (Fig. 1). The long-range ^{1}H–^{13}C correlations observed from H_2-18 to C-3, C-4, C-5, and the carbonyl carbon of 18-OAc further indicated the position of the epoxide at C-3 and C-4. The HMBC correlations from the vinylic methyl signal (H_3-19) correlated with those of an olefinic methine carbon (C-7), a methine carbon (C-9), and a quaternary olefinic carbon (C-8), led the location of the double bond at C-7 and C-8. The assignment of the secondary hydroxyl at C-9 was clarified by analysis of the above HMBC correlations (Fig. 1). In addition, the vinylic methyl signal (H_3-20) correlated with those of an olefinic methine carbon (C-11), a methylene carbon (C-13), and a quaternary olefinic carbon (C-12). The oxymethine proton at δ_H 5.28 was coupled to the olefinic CH at δ_H 5.52 (H-11) and correlated to C-20 and C-12, supporting C-11/C-12 unsaturation. The structure of **4** was generated by CS CHEM 3D version 9.0 using MM2 force field calculations for energy minimization, as shown in Figure 2. The result was consistent with the stereochemistry of **4** as established by the NOESY evidences and the computer-generated perspective modeling. NOE correlations between H-3/H-7, H-3/H-5a (δ 2.46), H-18a (δ 4.41)/H-5b (δ 1.23), H-7/H-5a, H-3/H-1, H-1/H-13, H-9/H-7, H-9/H-11, H-11/H-13, and H-14/H_3-20 confirmed the geometry of the *trans*-fused lactone ring and indicated that H-1, H-3, H-7, H-9, and H-11 are located on the same side of the ring system, whereas H-14, H_2-18, and H_3-20 are oriented toward the opposite side. The above findings also indicated the 1*R**, 3*R**, 4*S**, 9*S**, 13*R**, and 14*S** configurations as depicted in Figure 2. Thus, the structure of metabolite **4** was deduced as (1*R**,3*R**,4*S**,9*S**,13*R**,14*R**,7*E*,11*E*)-13,18-diacetoxy-9-hydroxy-3,4-epoxycembra-7,11,15(17)-trien-16,14-olide, which has been named durumolide I.

Table 3
^{1}H NMR spectroscopic data of metabolites 4–7

H#	**4**[a]	**5**[a]	**6**[b]	**7**[b]
1	2.82 m	2.77 m	3.06 m	3.12 dt (12.4, 2.4)[c]
2	a: 1.78 dt (14.4, 2.9)[c]	a: 1.87 dt (14.6, 2.4)[c]	a: 1.95 m	a: 2.12 m
	b: 1.56 m	b: 1.40 m	b: 1.78 m	b: 1.77 m
3	2.82 m	2.70 dd (7.3, 2.3)	3.04 m	3.35 dd (8.6, 2.4)
5	a: 2.46 m	a: 2.08 m	a: 2.13 m	a: 2.33 m
	b: 1.23 td (13.0, 2.6)	b: 1.24 m	b: 1.65 m	b: 2.01 ddd (12.8, 6.4, 4.0)
6	a: 2.35 m	a: 2.23 m	a: 2.18 m	a: 2.17 m
	b: 2.19 m	b: 2.10 m	b: 2.10 m	b: 2.15 m
7	5.37 br dd (9.6, 3.9)	5.03 br d (4.3)	5.18 br t (5.6)[c]	5.15 br t (6.0)
9	4.11 dd (10.4, 2.7)	a: 2.35 m	2.27 m	a: 2.32 m
		b: 2.12 m		b: 2.27 m
10	a: 2.67 m	a: 2.58 m	a: 2.58 m	a: 2.64 m
	b: 2.41 m	b: 2.52 m	b: 2.44 m	b: 2.42 m
11	5.52 br dd (8.3, 5.6)	5.47 br dd (9.7, 3.1)	6.68 t (6.8)	6.63 dd (6.8, 4.8)
13	5.28 d (8.5)	4.05 br s		
14	4.17 d (8.5)	4.06 d (6.0)	5.57 d (2.0)	5.51 d (2.0)
17	a: 6.33 d (2.9)	a: 6.32 d (3.2)	a: 6.28 d (2.0)	a: 6.34 d (2.0)
	b: 6.03 d (2.5)	b: 6.08 d (2.8)	b: 5.62 d (1.6)	b: 5.67 d (1.6)
18	a: 4.41 d (12.2)	1.24 s	a: 3.72 d (11.6)	9.42 s
	b: 3.85 d (12.2)		b: 3.67 d (11.6)	
19	1.71 s	1.64 s	1.62 s	1.61 s
20	1.72 s	1.73 s	1.84 s	1.86 s
18-OAc	2.15 s			
13-OAc	2.12 s			

[a] Spectra were measured in $CDCl_3$ (300 MHz).
[b] Spectra were measured in $CDCl_3$ (400 MHz).
[c] *J* values (in Hz) are in parentheses.

(1*R*,3*R*,4*R*,13*S*,14*R*,7*E*,11*E*)-13-hydroxy-3,4-epoxycembra-7,11,15(17)-trien-16,14-olide (**5**) was assigned a molecular formula of $C_{20}H_{28}O_4$, according to its HRESIMS and NMR spectroscopic data (Tables 2 and 3). A careful analysis of the NMR data coupled with COSY, HSQC, and HMBC correlations proved that the structure of **5** was identical to that of 13-acetoxy isolobophytolide[14] except for the presence of a hydroxyl instead of an acetoxy group at C-13. The NOE correlations (Fig. 2) between H-1/H-3, H-1/H-11, H-11/H-9, H-3/H-5a (δ_H 2.08), H_3-18/H-5b (δ_H 1.24), H-3/H-7, H-7/H-9, and H-14/H_3-20 indicated the relative configurations for the 14-membered ring carbons, which were identical to the same configuration as durumolide E[18] at the C-1, C-3, C-4, C-13, and C-14 stereocenters. In order to resolve the absolute stereochemistry of **5**, we determined the absolute configuration at C-13 using a modified Mosher's acylation.[22] The determination of $\Delta\delta_{S-R}$ values (Fig. 3) for the protons neighboring C-13 led to the assignment of the *R*-configuration at C-13 in **5**. Consequently, the structure of durumolide J (**5**) was established definitively.

The molecular formula of $C_{20}H_{26}O_5$ was assigned to metabolite **6** from its HRESIMS and ^{13}C NMR spectroscopic data (Table 2), indicating eight degrees of unsaturation. The NMR features (Tables 2 and 3) of **6** were analogous to those of **8**[19] except for the resonances in the vicinity of C-13. The exception was that the resonances for the methylene at C-13 were replaced by those of a keto group, consistent with the HMBC correlations (Fig. 1) from H_3-20 to C-11, C-12, and C-13. The computer-modeled structure of **6** was generated by CS CHEM 3D version 9.0 using MM2 force field calculations for energy minimization, as shown in Figure 2. The NOESY correlations (Fig. 2) between H-1/H-3, H-1/H-14, H-3/H-7, H-18a (δ_H 3.72)/H-5b (δ_H 1.65), H-7/H-9, H-14/H_3-20, and H-7/H-5a (δ_H 2.13) confirmed that H-1, H-3, and H-7 are located on the same side of the ring system, whereas H-14, H_2-18 and H_3-20 are oriented toward the opposite side. The above findings indicated the 1*R**, 3*R**, 4*S**, and 14*R** configurations as depicted in Figure 2. The *trans*-fused conformation of bicyclic ring junction was further supported by the coupling constant between the lactonic methine proton ($^3J_{1,14}$ = 2.0 Hz). In addition, the dihedral angle formed by H-

1, C-1, C-14, and H-14 is 109.9°, also indicating that H-1 and H-14 to be pseudoaxially and pseudoequatorially oriented, respectively. On the basis of the above observations, the structure of durumolide K (**6**) was assigned as (1*R**,3*R**,4*S**,14*R**,7*E*,11*E*)-18-hydroxy-13-oxo-3,4-epoxycembra-7,11,15(17)-trien-16,14-olide.

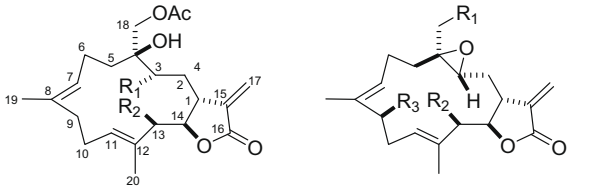

1 R_1= OH R_2= H
2 R_1= OAc R_2= OH
3 R_1= OAc R_2= OAc

4 R_1= OAc R_2= OAc R_3= OH
5 R_1= H R_2= OH R_3= H
8 R_1= OH R_2= H R_3=H

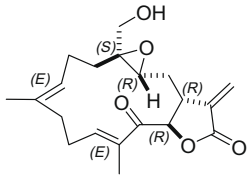

6

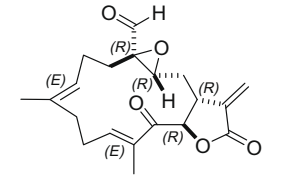

7

Durumolide L (**7**) analyzed for $C_{20}H_{24}O_5$ from HRESIMS and ^{13}C NMR spectroscopic data (Table 2), indicating nine degrees of unsaturation. The IR spectrum of **7** showed the presence of aldehyde (2846 and 1716 cm^{-1}), and α-methylene-γ-lactone (1776 and 1660 cm^{-1}) functionalities. The NMR features (Tables 2 and 3) of **7** were similar to those of **6**, except for the replacement of the hydroxymethyl by an aldehyde group [δ_H 9.42 (1H, s) and δC 199.3 (CH)] at C-4. This was supported by HMBC correlations from H-18 to C-3, C-4, and C-5, in a manner similar to that of **6**. The relative stereochemistry and the detailed ^1H NMR spectroscopic data assignment of **7** were determined mainly by the assistance of the NOESY experiment. The NOESY spectrum and the selected geometric parameters generated by CHEM3D PRO 9.0 and the coupling constant ($^3J_{1,14}$ = 2.0 Hz) indicated that **7** possessed the similar configurations for each ring junction and chiral center as **6** at C-1, C-3, C-4, and C-14. Therefore, metabolite **7** was definitely proposed as (1*R**,3*R**,4*R**,14*R**,7*E*,11*E*)-13,18-dioxo-3,4-epoxycembra-7,11,15(17)-trien-16,14-olide.

Geranylgeranyl pyrophosphate[23] is considered to be the precursor that, through a series of acid-catalyzed hydrolysis, cyclization, dehydrogenation, double bond rearrangement, epoxidation, hydroxylation, oxidation, and lactonization, would yield the cembranoids and their analogues isolated from marine soft corals. So far, it has been mentioned that almost all cembrane diterpenes of known absolute configuration at C-1 reported from the order Alcyonacea belong to the *R*-configuration (pointing downward), while the analogues isolated from the order Gorgonacea belong to the *S*-configuration.[24,25] Our results presented here have added further support to this conclusion.

The absolute stereochemistries of the cembranolides other than **1** and **5** remain to be determined because of the scarcity of material or the absence of secondary hydroxyl groups.

Metabolites **1**–**8** at a concentration of 100 μg/disk exhibited weak antibacterial activity against the bacterial strain, *Salmonella enteritidis* (ATCC13076). The results for inhibition of HCMV endonuclease activity assay are all negative at a concentration of 1 mg/mL.

Our previous study has reported that cembranolides possess iNOS (inducible nitric oxide synthetase) and COX-2 (cyclooxygenase-2) inhibition,[18] which prompted us to evaluate the anti-inflammatory effect of these isolated metabolites. As shown in Figure 4, the in vitro anti-inflammatory activity of metabolites **1**–**8** was tested using LPS-stimulated cells. Metabolites **1** and **6** significantly reduced the levels of the iNOS protein to 0.8 ± 0.6% and 5.7 ± 2.2%, respectively, and COX-2 protein to 47.8 ± 9.0% and 71.6 ± 5.8%, respectively, compare with the control cells (LPS alone) at a concentration of 10 μM. Under the same concentration, metabolites **2**–**5**, **7**, and **8** did not inhibit the COX-2 protein expression, but significantly inhibited iNOS protein expression to 7.3 ± 0.9%, 22.6 ± 4.9%, 6.2 ± 0.7%, 0.1 ± 0.1%, 1.2 ± 0.1%, and 2.2 ± 0.3%, respectively, by LPS stimulation. Moreover, the housekeeping protein β-actin was not changed by the presence of metabolites **1**–**8** at the same concentration. Under the same experimental conditions, 10 μM CAPE (caffeic acid phenylthyl ester) reduced the levels of the iNOS and COX-2 protein to 1.5 ± 2.1% and 70.2 ± 11.5%, respectively, relative to the control cells stimulated with LPS. The primary anti-inflammatory results suggested that the presence of α-methylene-γ-lactone functionality is required for the significantly activity against LPS-stimulated RAW 264.7 cells.

3. Experimental

3.1. General experimental procedures

Optical rotations were determined with a JASCO P1020 digital polarimeter. IR spectra were recorded on a JASCO FT/IR-4100 infrared spectrophotometer. UV spectra were obtained on a JASCO V-650 spectrophotometer. The NMR spectra were recorded on Bruker Avance 300 NMR/Varian MR 400 NMR/Varian Unity INOVA 500 FT-NMR spectrometers (300/400/500 MHz for ^1H and 75/100/125 MHz for ^{13}C), using $CDCl_3$ with TMS as internal standard. Chemical shifts are given in δ (ppm) and coupling constants in hertz. ESIMS were recorded by ESI FT-MS on a Bruker APEX II mass spectrometer. Si Gel 60 (Merck, 230–400 mesh) and LiChroprep RP-18 (Merck, 40–63 μm) were used for column chromatography. Precoated Si gel plates (Merck, Kieselgel 60 F_{254}, 0.25 mm) and precoated RP-18 F_{254s} plates (Merck) were used for analytical TLC analyses. High-performance liquid chromatography (HPLC) was carried out using a Hitachi L-7100 pump equipped with a Hitachi L-7400 UV detector at 220 nm and a semi-preparative reversed-phase column (Merck, Hibar Purospher RP-18e, 5 μm, 250 mm × 10 mm). *S*-(+)- and *R*-(−)-α-Methoxy-α-trifluoromethylphenylacetyl chloride were obtained from ACROS Organics (Geel, Belgium).

3.2. Animal materials

The soft coral *L. durum* was collected by hand using scuba at the Dongsha Islands located in northeastern South China Sea in April 2007, at a depth of 8 m, and was stored in a freezer for two months until extraction. This soft coral was identified by one of the authors (C.-F.D.). A voucher specimen (TS-13) was deposited in the Department of Marine Biotechnology and Resources, National Sun Yat-sen University.

3.3. Extraction and isolation

The frozen soft coral (1.2 kg) was chopped into small pieces and extracted with acetone for 24 h at room temperature. The quantity of solvent used for each extraction (2.0 L) was at least three times the amount of the soft coral material used (1.2 kg). The combined extracts were concentrated in vacuo (under 30 °C) to obtain 35.0 g of dry extract, which was suspended in water and extracted with EtOAc and *n*-BuOH (saturated with H_2O) sequentially. The EtOAc phase was evaporated to dryness in vacuo to give a brown residue (30.0 g). The resulting EtOAc residue was subjected to silica gel chromatography using a stepwise gradient mixture of *n*-hexane–EtOAc–MeOH as elution and separated into 40 fractions on the ba-

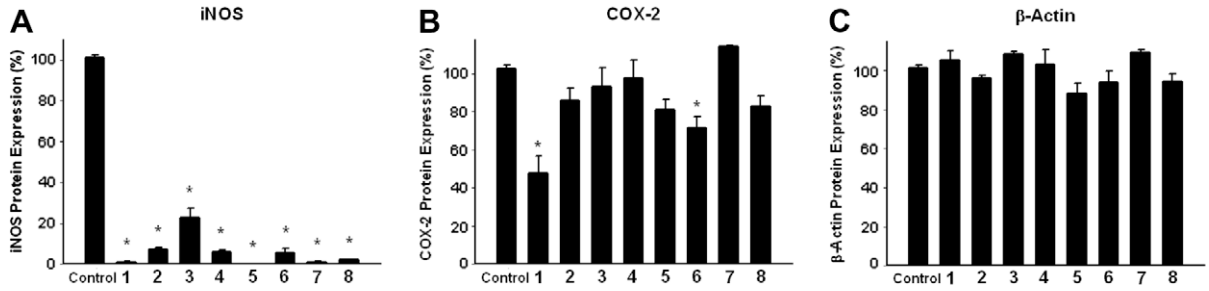

Figure 4. Effect of metabolites **1**–**8** at 10 μM on the LPS-induced pro-inflammatory iNOS and on COX-2 protein expression of RAW 264.7 macrophage cells by immunoblot analysis. (A) Immunoblot of iNOS; (B) Immunoblot of COX-2; (C) Immunoblot of β-actin. The values are mean ± S.E.M. (n = 5). The relative intensity of the LPS alone stimulated group was taken as 100%. * Significantly different from LPS-stimulated (control) group (* $P < 0.05$).

sis of TLC and ^{1}H NMR analysis. Fraction 19 (1.18 g) derived from the *n*-hexane–EtOAc (1:10) elution was subjected to a silica gel column using *n*-hexane–EtOAc mixtures of increasing polarity for elution, to afford 10 subfractions. A subfraction 19-3 (24 mg) eluted with *n*-hexane–EtOAc (2:1) was fractionated over Sephadex LH-20 (100% MeOH) to produce a mixture (16 mg) that was further purified by HPLC (RP-18) using 75% MeOH in H_2O to give **6** (1 mg) and **7** (1 mg). In turn, a subfraction 19-4 (60 mg) was applied to column chromatography on reversed-phase C_{18} gel column eluting with 70% MeOH in H_2O to afford a mixture (30 mg) that was further separated by HPLC (RP-18) using 65% MeOH in H_2O to provide **5** (4 mg) and **8** (18 mg). Similarly, a subfraction 19-5 (336 mg) eluted with *n*-hexane–EtOAc (1:2) was subjected to a RP-18 column eluting with 65% MeOH in H_2O to afford a mixture (214 mg) that was further purified by HPLC (RP-18) using 70% MeOH in H_2O to give **4** (2 mg). Metabolite **2** (1 mg) was obtained by separation of a subfraction 19-8 (48 mg) eluted with 100% EtOAc on a HPLC (RP-18) column eluting with 65% MeOH in H_2O. A subfraction 19-6 (202 mg) eluted with *n*-hexane–EtOAc (1:3) was subjected to column chromatography on reversed-phase C_{18} gel eluting with 65% MeOH in H_2O to yield a mixture (85 mg) that was further purified by HPLC (RP-18) using 70% MeOH in H_2O to give **1** (3 mg) and **3** (2 mg).

3.3.1. Durumolide F (1)

Colorless, viscous oil; $[\alpha]_D^{24}$ −61.3 (*c* 0.3, $CHCl_3$); UV (MeOH) λ_{max} (log ε) 216 (3.87) nm; IR (KBr) υ_{max} 3462, 2948, 1767, 1735, 1665, 1442, 1378, 1267, 1244, 1133, 1049, 952, 735 cm^{-1}; ^{1}H NMR and ^{13}C NMR data, see Tables 1 and 2; ESIMS *m/z* 415 $[M+Na]^+$; HRESIMS *m/z* 415.2097 $[M+Na]^+$ (calcd for $C_{22}H_{32}O_6Na$, 415.2096).

3.3.2. Durumolide G (2)

Colorless, viscous oil; $[\alpha]_D^{24}$ −32.6 (*c* 0.1, $CHCl_3$); UV (MeOH) λ_{max} (log ε) 214 (3.68) nm; IR (KBr) υ_{max} 3485, 2952, 1763, 1739, 1670, 1442, 1378, 1244, 1128, 1049, 952, 735 cm^{-1}; ^{1}H NMR and ^{13}C NMR data, see Tables 1 and 2; ESIMS *m/z* 473 $[M+Na]^+$; HRESIMS *m/z* 473.2153 $[M+Na]^+$ (calcd for $C_{24}H_{34}O_8Na$, 473.2152).

3.3.3. Durumolide H (3)

Colorless, viscous oil; $[\alpha]_D^{24}$ −36.5 (*c* 0.2, $CHCl_3$); UV (MeOH) λ_{max} (log ε) 215 (3.85) nm; IR (KBr) υ_{max} 3453, 2952, 1767, 1739, 1730, 1665, 1442, 1378, 1239, 1049, 952, 739 cm^{-1}; ^{1}H NMR and ^{13}C NMR data, see Tables 1 and 2; ESIMS *m/z* 515 $[M+Na]^+$; HRESIMS *m/z* 515.2259 $[M+Na]^+$ (calcd for $C_{26}H_{36}O_9Na$, 515.2257).

3.3.4. Durumolide I (4)

Colorless, viscous oil; $[\alpha]_D^{24}$ +48.3 (*c* 0.2, $CHCl_3$); UV (MeOH) λ_{max} (log ε) 217 (3.97) nm; IR (KBr) υ_{max} 3443, 2957, 1767, 1744, 1735, 1665, 1442, 1378, 1267, 1239, 1105, 1049, 957, 735 cm^{-1}; ^{1}H NMR and ^{13}C NMR data, see Tables 2 and 3; ESIMS *m/z* 471 $[M+Na]^+$; HRESIMS *m/z* 471.1993 $[M+Na]^+$ (calcd for $C_{24}H_{32}O_8Na$, 471.1995).

3.3.5. Durumolide J (5)

Colorless, viscous oil; $[\alpha]_D^{24}$ +6.7 (*c* 0.4, $CHCl_3$); UV (MeOH) λ_{max} (log ε) 215 (3.78) nm; IR (KBr) υ_{max} 3438, 2957, 1776, 1665, 1447, 1378, 1272, 1239, 1105, 1049, 943, 739 cm^{-1}; ^{1}H NMR and ^{13}C NMR data, see Tables 2 and 3; ESIMS *m/z* 355 $[M+Na]^+$; HRESIMS *m/z* 355.1886 $[M+Na]^+$ (calcd for $C_{20}H_{28}O_4Na$, 355.1885).

3.3.6. Durumolide K (6)

Colorless, viscous oil; $[\alpha]_D^{24}$ −118.0 (*c* 0.1, $CHCl_3$); UV (MeOH) λ_{max} (log ε) 236 (3.88), 210 (3.64) nm; IR (KBr) υ_{max} 3314, 2962, 1776, 1665, 1447, 1378, 1276, 1239, 1110, 1049, 947, 739 cm^{-1}; ^{1}H NMR and ^{13}C NMR data, see Tables 2 and 3; ESIMS *m/z* 369 $[M+Na]^+$; HRESIMS *m/z* 369.1680 $[M+Na]^+$ (calcd for $C_{20}H_{26}O_5Na$, 369.1678).

3.3.7. Durumolide L (7)

Colorless, viscous oil; $[\alpha]_D^{24}$ −160.4 (*c* 0.1, $CHCl_3$); UV (MeOH) λ_{max} (log ε) 235 (3.94), 210 (3.77) nm; IR (KBr) υ_{max} 2952, 2846, 1776, 1716, 1660, 1447, 1378, 1244, 1044, 952, 735 cm^{-1}; ^{1}H NMR and ^{13}C NMR data, see Tables 2 and 3; ESIMS *m/z* 367 $[M+Na]^+$; HRESIMS *m/z* 367.1361 $[M+Na]^+$ (calcd for $C_{20}H_{24}O_5Na$, 367.1362).

3.4. Preparation of (*R*)- and (*S*)-MTPA esters of 1 and 5

Duplicate (1.0 mg) samples of **1** were prepared for both (*R*)- and (*S*)-MTPA chloride acylation reactions. In separate vials, the samples were dissolved in 0.5 mL of dry pyridine and allowed to react overnight at room temperature with (*R*)- and (*S*)-MTPA chloride (one drop), respectively. The reaction was quenched by the addition of 1.0 mL of H_2O, followed by extraction with EtOAc (3 × 1.0 mL). The EtOAc-soluble layers were combined, dried over anhydrous $MgSO_4$ and evaporated. The residue of (*R*)-MTPA chloride acylation was subjected to a short silica gel column eluting with *n*-hexane–EtOAc (5:1) to yield (*S*)-MTPA ester **1a** (0.4 mg). The (*R*)-MTPA ester **1b** (0.3 mg) was prepared with (*S*)-MTPA chloride according to the same procedure as described above. In the same manner as shown above, two aliquots of **5** (1.0 mg) were dissolved in dry pyridine (0.5 mL) and allowed to react overnight with (*R*)- and (*S*)-MTPA chloride (one drop), affording the (*S*)-MTPA ester **5a** (0.4 mg) and (*R*)-MTPA ester **5b** (0.3 mg), respectively. Selected ^{1}H NMR($CDCl_3$, 400 MHz) of **1a**: δ_H 7.40–7.52 (5H, m, Ph), 6.21 (1H, d, *J* = 2.0 Hz, H-17a), 5.68 (1H, d, *J* = 2.0 Hz, H-17b), 5.22 (1H, t, *J* = 5.6 Hz, H-7), 5.16 (1H, t, *J* = 8.0 Hz, H-3), 5.07 (1H, br d, *J* = 5.2 Hz, H-11), 4.33 (1H, dt, *J* = 9.2, 3.2 Hz, H-14), 4.15 (1H, d, *J* = 11.6 Hz, H-18a), 4.08 (1H, d, *J* = 11.6 Hz, H-18b), 3.54 (3H, s, OCH3), 2.74 (1H, m, H-1), 2.46 (1H, br d, *J* = 11.6 Hz, H-13a), 2.08 (3H, s, 18-OAc), 2.04 (1H, m, H-5a), 2.01 (1H, m, H-2a), 1.73 (1H, m, H-5b), 1.67 (1H, m, H-2b), 1.66 (3H, s, Me-20), 1.64 (3H, s, Me-19); Selected ^{1}H NMR ($CDCl_3$, 400 MHz) of **1b**: δ_H 7.35–7.59 (5H, m, Ph), 6.20 (1H, d, *J* = 2.0 Hz, H-17a), 5.65 (1H, d, *J* = 2.0 Hz, H-17b), 5.25 (1H, t, *J* = 5.6 Hz, H-7), 5.18 (1H, t,

J = 8.0 Hz, H-3), 5.08 (1H, br d, J = 5.2 Hz, H-11), 4.44 (1H, dt, J = 9.2, 3.2 Hz, H-14), 4.14 (1H, d, J = 11.6 Hz, H-18a), 4.07 (1H, d, J = 11.6 Hz, H-18b), 3.45 (3H, s, OCH3), 2.92 (1H, m, H-1), 2.44 (1H, br d, J = 11.6 Hz, H-13a), 2.05 (3H, s, 18-OAc), 2.05 (1H, m, H-2a), 2.00 (1H, m, H-5a), 1.72 (1H, m, H-5b), 1.69 (1H, m, H-2b), 1.64 (3H, s, Me-20), 1.62 (3H, s, Me-19). Selected ^{1}H NMR ($CDCl_3$, 400 MHz) of **5a**: δ_H 7.41–7.57 (5H, m, Ph), 6.33 (1H, d, J = 3.2 Hz, H-17a), 6.03 (1H, d, J = 3.2 Hz, H-17b), 5.63 (1H, br t, J = 6.0 Hz, H-11), 5.38 (1H, br d, J = 8.8 Hz, H-7), 5.28 (1H, d, J = 8.8 Hz, H-13), 4.11 (1H, dd, J = 10.8, 2.8 Hz, H-14), 3.55 (3H, s, OCH3), 2.94 (1H, m, H-1), 2.82 (1H, m, H-3), 1.74 (3H, s, Me-20), 1.72 (3H, s, Me-19), 1.26 (3H, s, Me-18); Selected ^{1}H NMR($CDCl_3$, 400 MHz) of **5b**: δ_H 7.40–7.58 (5H, m, Ph), 6.34 (1H, d, J = 3.2 Hz, H-17a), 6.03 (1H, d, J = 3.2 Hz, H-17b), 5.52 (1H, br t, J = 6.0 Hz, H-11), 5.37 (1H, br d, J = 8.8 Hz, H-7), 5.17 (1H, d, J = 8.8 Hz, H-13), 4.16 (1H, dd, J = 10.8, 2.8 Hz, H-14), 3.55 (3H, s, OCH3), 2.95 (1H, m, H-1), 2.83 (1H, m, H-3), 1.72 (3H, s, Me-20), 1.71 (3H, s, Me-19), 1.26 (3H, s, Me-18).

3.5. Molecular mechanics calculations

Implementation of the MM2 force field[26] in CHEM3D PRO software from CambridgeSoft Corporation, Cambridge, MA, USA (ver. 9.0, 2005), was used to calculate molecular models.

3.6. Antimicrobial activity

Bacterial strains were grown in LB (Luria-Bertani) broth medium for 24 h at 37 °C. Then, 17 mL LB hard agar (1.5% agar) was poured into sterile Petri dishes (9 cm) and allowed to set. Next, 2.7 mL molten LB soft agar (0.7% agar, 45 °C) was inoculated with 0.3 mL broth culture of the test organism and poured over the base hard agar plates forming a homogenous top layer. Sterile paper disks (Advantec, 8 mm) were placed onto the top layer of the LB agar plates. Ten milliliters (2 μg/μL) of the tested compounds were applied on to each the filter paper disks. Ampicillin (5 μg/μL) and the same solvents were served as positive and negative controls. All plates were incubated at 37 °C, 24 h prior to antibacterial activity evaluation. The antimicrobial activity of all isolated metabolites **1**–**8** was tested up to 100 μg/disk on *S. enteritidis* (ATCC13076). The bacterial strain was obtained from the American Type Culture Collection. The antibiotic activity evaluation method was conducted based on previously reports.[27,28]

3.7. Anti-inflammatory assay

The anti-inflammatory assay was modified from Ho et al.[29] and Park et al.[30] Murine RAW 264.7 macrophages were obtained from the American Type Culture Collection (ATCC, No. TIB-71). The cells were activated by incubation in medium containing *Escherichia coli* LPS (0.01 μg/mL; Sigma) for 16 h in the presence or absence of various compounds. Then, cells were washed with ice-cold PBS, lysed in ice cold lysis buffer, and centrifuged at 20,000*g* for 30 min at 4 °C. The supernatant was decanted from the pellet and retained for Western blot analysis. Protein concentrations were determined by the DC protein assay kit (Bio-Rad) modified by the method of Lowry et al.[31] Samples containing equal quantities of protein were subjected to SDS–polyacrylamide gel electrophoresis, and the separated proteins were electrophoretically transferred to polyvinylidene difluoride membranes (PVDF; Immobilon-P, Millipore, 0.45 μm pore size). The resultant PVDF membranes were incubated with blocking solution and incubated for 180 min with antibody against inducible nitric oxide synthase (iNOS; 1:1000 dilution; Transduction Laboratories) and cyclooxygenase-2 (COX-2; 1:1000 dilution; Cayman Chemical) protein. The blots were detected using ECL detection reagents (Perkin–Elmer, Western Blot Chemiluminescence Reagent Plus) according to the manufacturer, *Sigma Chemical Company*, *St. Louis*, *MO*, mark an inner of CAPE in var. paragraph instructions.

3.8. Inhibition of endonuclease activity assay

The HCMV UL76 encodes an endonuclease[32] was purified from *E. coli* BL21-codon DE3-RIL strain, which was transformed with calmodulin-tagged UL76 plasmid pCBP-UL76. The double-stranded supercoiled DNA φX174 was purified by CsCl gradient and used as substrate.[33] Tested compounds were series diluted and incubated with 1 μg DNA substrate, reaction buffer and UL76 endonuclease at 37 °C for 1 h. After cleavage reaction, DNA was resolved in 1% agarose gel. Concentrations of tested compounds that exert 50% of inhibition of cleaved substrate (IC_{50}) were recorded.

Acknowledgments

This work was supported by grants from the Ministry of Education (97C031703) and National Science Council (NSC96-2320-B-110-003-MY3) of the Republic of China awarded to C.-Y.D.

References and notes

1. Blunt, J. W.; Copp, B. R.; Hu, W. P.; Munro, M. H. G.; Northcote, P. T.; Prinsep, M. R. *Nat. Prod. Rep.* **2008**, *25*, 35.
2. Higuchi, R.; Miyamoto, T.; Yamada, K.; Komori, T. *Toxicon* **1998**, *36*, 1703.
3. Matthee, G. F.; Konig, G. M.; Wright, A. D. *J. Nat. Prod.* **1998**, *61*, 237.
4. Wang, S. K.; Duh, C. Y.; Wu, Y. C.; Wang, Y.; Cheng, M. C.; Soong, K.; Fang, L. S. *J. Nat. Prod.* **1992**, *55*, 1430.
5. Coval, S. J.; Patton, R. W.; Petrin, J. M.; James, L.; Rothofsky, M. L.; Lin, S. L.; Patel, M.; Reed, J. K.; McPhil, A. T.; Bishop, W. R. *Bioorg. Med. Chem. Lett.* **1996**, *6*, 909.
6. Duh, C. Y.; Wang, S. K.; Huang, B. T.; Dai, C. F. *J. Nat. Prod.* **2000**, *63*, 884.
7. Yamada, K.; Ryu, K.; Miyamoto, T.; Higuchi, R. *J. Nat. Prod.* **1997**, *60*, 798.
8. Subrahmanyam, C.; Rao, C. V.; Anjaneyulu, V.; Satyanarayana, P.; Rao, P. V. S. *Tetrahedron* **1992**, *48*, 3111.
9. Bowdon, B. F.; Coll, J. C.; Heaton, A.; Konig, G.; Bruck, M. A.; Cramer, R. E.; Klein, D. M.; Scheuer, P. J. *J. Nat. Prod.* **1987**, *50*, 650.
10. Uchio, Y.; Eguchi, S.; Kuramoto, J.; Nakayama, M.; Hase, T. *Tetrahedron Lett.* **1985**, *26*, 4487.
11. Tursch, B.; Braekman, J. C.; Daloze, D.; Herin, M.; Karlsson, R. *Tetrahedron Lett.* **1974**, *43*, 3769.
12. Kashman, Y.; Groweiss, A. *Tetrahedron Lett.* **1977**, *13*, 1159.
13. Kinamoni, Z.; Groweiss, A.; Carmely, S.; Kashman, Y. *Tetrahedron* **1983**, *39*, 1643.
14. Kashman, Y.; Carmely, S.; Groweiss, A. *J. Org. Chem.* **1981**, *46*, 3592.
15. Rashid, M. A.; Gustafson, K. R.; Boyd, M. R. *J. Nat. Prod.* **2000**, *63*, 531.
16. Bowden, B. F.; Coll, J. C.; Tapiolas, D. M. *Aust. J. Chem.* **1983**, *36*, 2289.
17. Bowden, B. F.; Coll, J. C.; Decosta, M. S. L.; Desilva, E. D.; Mackay, M. F.; Mahendran, M.; Willis, R. H. *Aust. J. Chem.* **1984**, *34*, 545.
18. Cheng, S. Y.; Wen, Z. H.; Chiou, S. F.; Wang, S. K.; Hsu, C. H.; Dai, C. F.; Chiang, M. Y.; Duh, C. Y. *Tetrahedron* **2008**, *64*, 9698.
19. Zhang, W.; Krohn, K.; Ding, J.; Miao, Z. H.; Zhou, X. H.; Chen, S. H.; Pescitelli, G.; Salvadori, P.; Kurtan, T.; Guo, Y. W. *J. Nat. Prod.* **2008**, *71*, 961.
20. Li, G.; Zhang, Y.; Deng, Z.; van Ofwegen, L.; Proksch, P.; Lin, W. *J. Nat. Prod.* **2005**, *68*, 649.
21. Iwashima, M.; Matsumoto, Y.; Takenaka, Y.; Iguchi, K.; Yamori, T. *J. Nat. Prod.* **2002**, *65*, 1441.
22. Ohtani, I.; Kusumi, T.; Kashman, Y.; Kakisawa, H. *J. Am. Chem. Soc.* **1991**, *113*, 4092.
23. Kinamoni, Z.; Groweiss, A.; Carmely, S.; Kashman, Y.; Loya, Y. *Tetrahedron* **1983**, *39*, 1643.
24. Rodriguez, A. D.; Li, Y.; Dhasmana, H.; Barnes, C. *J. Nat. Prod.* **1993**, *56*, 1101.
25. Pham, N. B.; Butler, M. S.; Quinn, R. J. *J. Nat. Prod.* **2002**, *65*, 1147.
26. Allinger, N. L. *J. Am. Chem. Soc.* **1977**, *99*, 8127.
27. Hou, L.; Shi, Y.; Zhai, P.; Le, G. *J. Ethnopharmacol.* **2007**, *111*, 227.
28. Arias, M. E.; Gomez, J. D.; Cudmani, N. M.; Vattuone, M. A.; Isla, M. I. *Life Sci.* **2004**, *75*, 191.
29. Ho, F. M.; Lai, C. C.; Huang, L. J.; Kuo, T. C.; Chao, C. M.; Lin, W. W. *Br. J. Pharmacol.* **2004**, *141*, 1037.
30. Park, E. K.; Shin, Y. W.; Lee, H. U.; Kim, S. S.; Lee, Y. C.; Lee, B. Y.; Kim, D. H. *Biol. Pharm. Bull.* **2005**, *28*, 652.
31. Lowry, D. H.; Rosebrough, N. J.; Farr, A. L.; Randall, R. J. *J. Biol. Chem.* **1951**, *193*, 265.
32. Knizewski, L.; Kinch, L.; Grishin, N. V.; Rychlewski, L.; Ginalski, K. *J. Virol.* **2006**, *80*, 2575.
33. Tachiwana, H.; Shimura, M.; Nakai-Murakami, C.; Tokunaga, K.; Takizawa, Y.; Sata, T.; Kurumizaka, H.; Ishizaka, Y. *Cancer Res.* **2006**, *66*, 627.